Journal of Applied Polymer Science

Synthesis of Two D-π-A Polymers π-Bridged by Different Blocks and Investigation of Their Photovoltaic Property

Ruiping Qin, Yurong Jiang, Kaixuan Zhang, Haoxing Zhang, Qunying Zhang, Meng Li, Heng Ma
College of Physics & Electronic Engineering, Key Laboratory of Photovoltaic Materials of Henan Province, Henan Normal University, Xinxiang 453007, China
Correspondence to: R. Qin (E-mail: qinruiping@163.com)

ABSTRACT: The synthesis, characterization, photophysical and photovoltaic properties of two 5,6-bis(octyloxy)benzo[c][1,2,5]thiadiazole-containing wide-band-gap donor and acceptor D-π-A alternating conjugated polymers (HSD-a and HSD-b) have been reported. These two polymers absorb in the range of 300–700 nm with a band gap of about 1.88 and 1.97 eV. The HOMO energy levels were −5.44 eV for HSD-a and −5.63 eV for HSD-b. Polymer solar cells with HSD-b :$PC_{71}BM$ as the active layer demonstrated a power conversion efficiency (PCE) of 2.59% with a high V_{oc} of 0.93 V, a J_{sc} of 7.3 mA/cm^2, and a comparable fill factor (FF) of 0.38 under simulated solar illumination of AM 1.5G (100 mW/cm^2) without annealing. In addition, HSD-a :$PC_{71}BM$ blend-based solar cells exhibit a PCE of 2.15% with a comparable V_{oc} of 0.64 V, J_{sc} of 8.75 mA/cm^{-2}, and FF of 0.40. © 2014 Wiley Periodicals, Inc. J. Appl. Polym. Sci. **2015**, *132*, 41587.

KEYWORDS: conducting polymers; optical and photovoltaic applications; properties and characterization

Received 4 June 2014; accepted 1 October 2014
DOI: 10.1002/app.41587

INTRODUCTION

Recently, the harvesting of solar energy by polymer solar cells (PSCs) has attracted considerable attention for their unique advantages of reducing the price and environmental impact.[1–4] An effective approach to realize high power conversion efficiencies (PCEs) for PSCs was the design and preparation of alternating donor and acceptor (D–A) structure polymers.[5–8] New organic materials, novel solar cell device structures, and optimization of film morphology of active layers have led to a dramatic increase of PCE in Bulk heterojunction (BHJ) PSCs. PCE higher than 9% has been achieved.[9–11] Perovskite solar cells also brought about a skyrocket PCE.[12–14] Recently, the company Heliatek reported a high efficiency of 12.0% for small molecule tandem solar cells.[15] A tandem or Triple-Junction structure device shows an inspiring approach to realize high efficiency. In the tandem solar cell, a wide-band-gap material always as the front cell and a low-band-gap material-based rear cell are stacked in series to jointly absorb a wide range of the solar spectrum. It is an important strategy to obtain a proper matched wide-band-gap (~2.0 eV) materials for the front cell and low-band-gap (~1.5 eV) materials for the rear cell.[16] The open-circuit voltage (V_{oc}) of the tandem structure is equal to the sum of V_{oc} of two individual cells and the short-circuit current density (J_{sc}) is determined by the current density of the lower. Deep highest occupied molecular orbital (HOMO) energy level is an important parameter both for device stability and a maximization value of V_{oc} for PSCs.[17] Poly(3-hexylthiophene) (P_3HT) is the most commonly used wide-band-gap material for the tandem solar cells. However, this homopolymers has a −4.76 eV HOMO energy level and narrow absorption spectra. The high-lying HOMO value usually leads to lower the total V_{oc} of tandem PSCs.[18] For this reason, it is necessary to develope new materials with a suitable energy level. Insert different π-bridge between alternating donor and acceptor blocks can fine-tuning the absorption spectra and energy levels of the resultant polymers.[19] Therefore, designing and synthesizing highly efficient wide-band-gap conjugated materials with deep HOMO level are extremely important for achieving high efficiency tandem solar cells. The carbazole unit is a widely used donor material in conductive polymers for its planar molecular configuration and electron rich nature. Carbazole-based polymers are of deep HOMO energy level. The HOMO energy levels are typically in the −5.2 to −5.8 eV range as being necessary deep energy level for donors in high efficiency BHJ cells.[20] This suggests that carbazole-based polymers with appropriate band gaps might be extremely good photovoltaic materials. Among the carbazoles class, 2,7-linked carbazole units are more π-expanded systems and easy constructed as "molecular wires".[21] Some high efficiency carbazole contained D−A copolymers

Additional Supporting Information may be found in the online version of this article.

reported in literatures could be improved further by inserting suitable π-bridges.[22,23] However, unmatched conjugated units will result in notable large dihedral angle along the main chain. Large torsion angle will destroy the electronics delocalization of the polymer backbone.[24] This will narrow the light absorption range of the active layer. The relatively narrow absorption spectrum and less effective conjugation in the main chain are the critical factors that limit the improvement of photoelectric properties. It is obviously a failure strategy that a donor block polymerized with an accept block directly to prepare photovoltaic material like HSD-C (Supporting Information Figures S12 and S13). A larger dihedral angle destroyed the electronics delocalization result in a dramatically blue shift and low absorbs ability. The absorption spectra are far away from that range of solar maximum photons emission. It is a reasonable strategy to adapt the polymer absorption spectra match better with solar energy by choosing a proper electron-rich block as pi-bridge between the donors and acceptors so that it is able to adjust the coplanarity or enlarge electronics delocalization.

In this article, the authors designed and synthesized two D-π-A alternating conjugated polymers with 2,7-linked carbazole as donor unit and 5,6-bis(octyloxy)benzo[*c*][1,2,5] thiadiazole as acceptor unit bridged by bithiophene or 3-undecylthieno[3,2-*b*]thiophene. It was found that series and fused thiophene in the copolymer are able to significantly affect the properties of the polymers. Different conjugated bridges crucially influence the electron delocalization of polymer main chain and the interactions in the active layer; therefore remarkably affect film morphology and consequently optical, electrochemical, charge transport and photovoltaic properties of the D-π-A conjugated copolymers. Thus, it is of prime importance to fully understand the structure-property of different π-bridge polymers on the physicochemical and photovoltaic properties for the design of high efficient new polymers.

EXPERIMENTAL

Reagents and Instruments

Solvents were dried using standard procedures. Material M1[1]; M4[25]; M5[26]; M8[21] were synthesized according to literature procedures. The catalyst precursor $Pd(PPh_3)_4$ was prepared according to the literature and stored in a Schlenk tube under nitrogen.[27] Unless otherwise noted, all chemicals were purchased from commercial suppliers and used without further purification. ^{1}H- and ^{13}C-NMR was recorded on a Bruker AV400 spectrometer in $CDCl_3$. Electronic absorption were obtained on a Shimadzu model UV-3600 PC ultraviolet–visible (UV–vis) spectrometer. Elemental analyses were performed on a Flash EA1112 analyzer. Powder X-ray diffraction (XRD) patterns were obtained by Cu KR radiation on a PANalytical X′ Pert PROMPD diffract meter. The electrochemical behavior were investigated by cyclic voltammeter (CHI 630A Electrochemical Analyzer) use a standard three-electrode electrochemical cell, in a 0.1*M* tetrabutylammonium Hexafluorophosphate solution in CH_3CN, at room temperature and at N_2 atmosphere with a scanning rate of 0.1 V/S. A glassy carbon working electrode, a Pt wire counter electrode, and an $Ag/AgNO_3$ (0.01*M* in CH_3CN) reference electrode were used. The experiments were calibrated with the standard ferrocene/ferrocenium (Fc) redox system, assuming that the energy level of Fc is 4.8 eV below vacuum. The thermal gravimetric analysis (TGA) was carried out under a nitrogen atmosphere using a NETZSCH STA 449C instrument with a heating rate of 10°C/min to record trace. SEM was performed on a SUPRA^{TM} 40 electron microscope (FEI) operated at 15 KV.

Polymer Solar Cell Fabrication and Characterization

PSCs were fabricated with the device configuration of ITO/PEDOT : PSS/Polymer : $PC_{71}BM$ /LiF/Al. The conductivity of ITO was 20 Ω/□. PEDOT : PSS is Baytron AI 4083 from H.C.Starck and was filtered with a 0.45 mm PVDF film before use. A thin layer of PEDOT:PSS was spin-coated on top of cleaned ITO substrate at 3000 rpm/s for 60 s and dried subsequently at 120°C for 20 min on a hotplate before transferred into a glove box. The thickness of the PEDOT : PSS layer was about 40 nm. The blend of polymers and $PC_{71}BM$ was dissolved in ODCB and heated at 90°C for overnight to ensure the sufficient dissolution, and then spin-coated onto PEDOT : PSS layer. The top electrode was thermally evaporated, with a 0.6 nm LiF layer, followed by 100 nm of aluminum at a pressure of 10^{-4} Pa through a shadow mask. Five cells were fabricated on one substrate with an effective area of 0.04 cm^2. The measurement of devices was conducted in air without encapsulation. Current-voltage characteristics were recorded use a Keithley 2400 Source meter under an AM1.5G AAA class solar simulator (model XES-301S, SAN-EI) with intensity of 100 mW/cm^2 as the white light source and the intensity was calibrated with a standard single-crystal Si photovoltaic cell. The temperature while measuring the *J-V* curves was approximately 25°C.

Preparation of Monomers

4,7-Di(2,2′-bithiophen-5-yl)-5,6-bis(octyloxy)benzo [c][1,2,5]thiadiazole (M2). A mixture of M1 (0.5 g, 0.76 mmol) and 4,4,5,5-tetramethyl-2-(thiophen-2-yl)-1,3,2-dioxaborolane (0.4 g, 1.9 mmol), Na_2CO_3 (1.0 g, 9.4 mmol), toluene (25 mL), and water (5 mL) was carefully degassed before and after $Pd(PPh_3)_4$ (0.1 g, 0.086 mmol) was added. The reaction mixture was stirred at 90°C under nitrogen atmosphere for 3 days. The organic layer was separated; the aqueous layer was extracted with CH_2Cl_2 (3× 10 mL); the combined organic layers were dried over anhydrous Na_2SO_4 and evaporated to dryness. The residue was chromatographically purified on silica gel column eluting with CH_2Cl_2/hexane (1 : 10, v : v) to afford M2 as red crystal (0.49 g, 97%).

^{1}H NMR (400 MHz, $CDCl_3$, δ): 8.42–8.41 (*d*, $J = 3.84$ Hz, 2H), 7.22–6.92 (m, 8H), 4.10-4.07 (*t*, $J = 6.96$Hz, 4H), 1.95–1.87 (m, 4H), 1.42–1.39 (m, 4H), 1.27–1.18 (m, 16H), 0.82–0.76 (*t*, $J = 5.59$ Hz, 6H).

^{13}C NMR (100 MHz, $CDCl_3$, δ): 151.84, 151.01, 139.09, 137.81, 133.38, 131.85, 128.14, 124.84, 123.95, 123.78, 117.50, 74.76, 32.06, 30.66, 29.79, 29.54, 26.29, 22.90, 14.32. Anal. Calcd. for $C_{38}H_{44}N_2S_5$: C, 63.29; H, 6.15; N, 3.88. Found: C, 63.22; H, 6.25; N, 4.25. MALDI-TOF, m/z: calcd, 720.20; found, 720.3 (M^+).

4,7-Bis(5′-bromo-2,2′-bithiophen-5-yl)-5,6-bis(octyloxy)benzo[c][1,2,5]thiadiazole (M3). A mixture of M2 (0.4 g, 0.55 mmol), *N*-bromosuccimide (NBS) (0.20 g, 1.13 mmol), and chloroform

(50 mL) was stirred at room temperature in dark for 24 h. The solvent was removed under reduced pressure, the residue was chromatographically purified on silica gel column eluting with CH_2Cl_2/hexane (1 : 20, v : v) to afford M3 as red crystal (0.46 g, 94%).

^{1}H NMR (400 MHz, $CDCl_3$, δ): 8.49-8.48 (*d*, $J = 3.40$ Hz, 2H), 7.23-7.22 (*d*, $J = 4.00$ Hz,2H), 7.03–7.00 (dd, $J = 3.88$ Hz, 4H), 4.17-4.14 (*t*, $J = 7.04$ Hz,4H), 2.0–1.93 (m, 4H), 1.51-1.45 (m, 4H), 1.34-1.29 (m, 16H), 0.90-0.87 (*t*, $J = 6.40$ Hz, 6H).

^{13}C NMR (100 MHz, $CDCl_3$, δ): 151.80, 150.84, 139.31, 137.94, 133.76, 131.86, 130.97, 128.55, 123.92, 117.38, 111.45, 74.76, 32.08, 30.67, 29.80, 29.56, 26.31, 22.93, 14.34. Anal. Calcd. for $C_{38}H_{42}Br_2N_2O_2S_5$: C, 51.93; H, 4.82; N, 3.19. Found: C, 52.10; H, 4.82; N, 3.18.

5,6-Bis(octyloxy)-4,7-bis(6-undecylthieno[3,2-b]thiophen-2-yl)benzo[c][1,2,5]thiadiazole (M6). M4 (5.9 g, 13mmol) was added to a stirring mixture of M5 (3.2 g, 5.9 mmol), DMF (10 mL), toluene (80 mL), $Pd(PPh_3)_4$ (68.1 mg, 0.059 mmol), and CuI (7.6 mg, 0.040 mmol). After the solution was stirred for 12 h at 80°C, CH_2Cl_2 (200 mL) was added to the solution. The organic layer was washed with water (3× 200 mL) and dried over anhydrous Na_2SO_4. After removing the solvent in vacuum, the residue was purified by column chromatography on silica gel (hexanes)) to yield M6 (3.0 g, 52%) as red solid.

^{1}H NMR (400 MHz, $CDCl_3$, δ:) 8.77 (s, 2H), 7.06 (s, 2H), 4.19-4.16 (*t*, $J = 7.20$ Hz,4H), 2.82-2.78 (*t*, $J = 7.60$ Hz, 4H), 2.05-1.97 (m, 4H), 1.88-1.80(m, 4H), 1.55-1.29 (m, 52H), 0.94-0.89(m, 12H). ^{13}C NMR (100 MHz, $CDCl_3$, δ:) 151.84, 150.82, 147.73, 138.70, 135.59, 135.06, 123.56, 122.90, 118.03, 74.74, 32.02, 31.96, 30.57, 30.13, 29.80, 29.76, 29.61, 29.47, 29.43, 28.81, 26.20, 22.79, 14.21.

4,7-Bis(5-bromo-6-undecylthieno[3,2-b]thiophen-2-yl)-5,6-bis(octyloxy)benzo[c][1,2,5]thiadiazoe (M7). M6 (1.32 g, 1.35mmol) was dissolved in 200 mL solvent (100 mL DMF/100 chloroform); *N*-bromosuccimide (NBS) (0.49 g, 2.77 mmol) was added at room temperature. The mixture was heated to 80°C for 1h and cooled down to room temperature. 300 mL H_2O was added. The aqueous layer was extracted with chloroform (3× 30 mL). The organic layer was dried over anhydrous Na_2SO_4 and the solvent was removed under vacuum until 50 mL was left. The residue was poured and stirred into 200 mL methanol; the resulted precipitate was collected by filtration and washed with methanol (3 x 10 mL). The title compound was got as a red power. 1.41g (Yield: 94%).^{1}H NMR (400 MHz, $CDCl_3$, δ:) 8.72 (s, 2H), 4.17-4.14 (*t*, $J = 7.20$ Hz,4H), 2.81-2.78 (*t*, $J = 7.60$Hz, 4H), 1.99-1.95 (m, 4H), 1.80-1.77(m, 4H), 1.50-1.26 (m, 52H), 0.91-0.85(m, 12H). ^{13}C NMR (100 MHz, $CDCl_3$, δ:) 151.78, 150.69, 140.29, 136.98, 134.89, 134.29, 122.94, 117.79, 111.49, 74.83, 31.96, 31.90, 30.52, 29.74, 29.70, 29.67, 29.53, 29.45, 29.40, 29.25, 28.17, 26.14, 22.73, 14.16.

Preparation of Polymers

HSD-a, a mixture of M8 (0.30 g, 0.46 mmol), M3 (0.41 g, 0.46 mmol), THF (45 mL), Toluene (15 mL), H_2O (9 mL), $NaHCO_3$ (1.8 g, 21.6 mmol) was carefully degassed before and after $Pd(PPh_3)_4$ (15 mg, 14 μmol) was added. The mixture was stirred and refluxed for 2 days under nitrogen. Phenylboronic acid (10 mg, 0.08 mmol) was added; the reaction was further refluxed for 12 h; then 1-bromobenzene (0.05 mL, 0.48 mmol) was added; and the reaction was refluxed for another 12 h. When it cooled to room temperature, the mixture was poured into methanol (200 mL) and the resulted precipitate was collected by filtration. The crude polymer was dissolved in hot chloroform (300 mL) and filtered. The filtration was concentrated to about 50 mL and precipitated into acetone (400 mL). The precipitated was collected by filtration and dried under high vacuum to afford polymer HSD-a as a black solid (0.36 g, yield: 69%). A number average molecular weight (Mn) of 17.8 kg/mol, a weight average molecular weight (Mw) of 53.0 kg/mol, and a polydispersity index (PDI) of 2.96 were determined by gel permeation chromatography (GPC) at 150°C with 1,2,4-trichlorobenzene as an eluant vs polystyrene standards on a PL-GPC 220. ^{1}H NMR (400 MHz, $CDCl_3$, δ:) δ 8.28-8.26 (m, 2H), 8.07-7.14 (m, 12H), 3.94-3.81 (m, 6H), 1.92-1.84 (m, 4 H), 1.60-1.30 (m, 32 H), 0.60 (m, 9H). ^{13}C NMR (100 MHz, solid state): δ 150.73, 144.26, 141.76, 137.69, 132.49, 122.57, 117.42, 105.75, 73.69, 30.98, 23.56, 14.85. Anal. Calcd. for $[C_{66}H_{83}N_3O_2S_5]_n$: C, 71.37; H, 7.53; N, 3.78. Found: C, 71.27; H, 7.46; N, 4.24.

HSD-b, the synthesis of HSD-b was similar to HSD-a. M8 (0.47 g, 0.88 mmol), M7 (1.0 g, 0.88 mmol), THF (150 mL), Toluene (50 mL), H_2O (30 mL), $NaHCO_3$ (6.0 g, 70 mmol) and $Pd(PPh_3)_4$ (30 mg, 28 μmol) was used. 1.071 g polymer HSD-b was obtained as a black solid (yield: 96%).

A Mn of 18.92 kg/mol, a Wm of 23.0 kg/mol, and a PDI of 1.23 were determined by gel permeation chromatography (GPC) at 35°C with THF as eluant vs polystyrene standards on a Waters chromatography connected to a Water 410 differential refractive index meter.

^{1}H NMR (400 MHz, $CDCl_3$, δ:) δ 8.85 (s, 2H), 8.15 (s, 2H), 7.56-7.42(m, 4H), 4.25-4.22 (m, 8H), 3.00–2.96 (m, 8 H), 2.09-1.35 (m, 52 H), 0.88 (m, 12H). ^{13}C NMR (100 MHz, $CDCl_3$, δ:) 143.43, 141.08, 136.82, 134.93, 132.80, 130.81, 123.40, 120.78, 118.02, 102.09, 100.01, 31.95,30.63, 29.78, 29.73, 29.64, 29.52, 29.41, 29.30, 28.83, 26.61, 22.72, 22.67, 14.14.

RESULTS AND DISCUSSION

The syntheses routes and characterization datas of monomers and corresponding polymers are outlined in Scheme 1 and Supporting Information Figures S14–S17. Suzuki–Miyaura cross-coupling reaction for M1 and 4,4,5,5-tetramethyl- 2-(thiophen-2-yl)-1,3,2-dioxaborolane was carried out in a biphasic mixture of THF and aqueous $NaHCO_3$ with $Pd(PPh_3)_4$ as the catalyst to afford M2 in a yield of 97%. Brominating of M2 with *N*-bromosuccinimide furnished M3 in a yield of 94%. M6 was obtained in a modest yield of 52% by palladium-catalyzed Stille cross-coupling reaction. Brominating of M6 in a mixture of chloroform and *N*, *N*-Dimethylformamide (DMF) (v/v: 1/1) afforded M7 in a yield of 94%. Polymers HSD-a and HSD-b were synthesized by Suzuki polycondensation of M8 with M3 and with M7, respectively. The polymerization was carried out

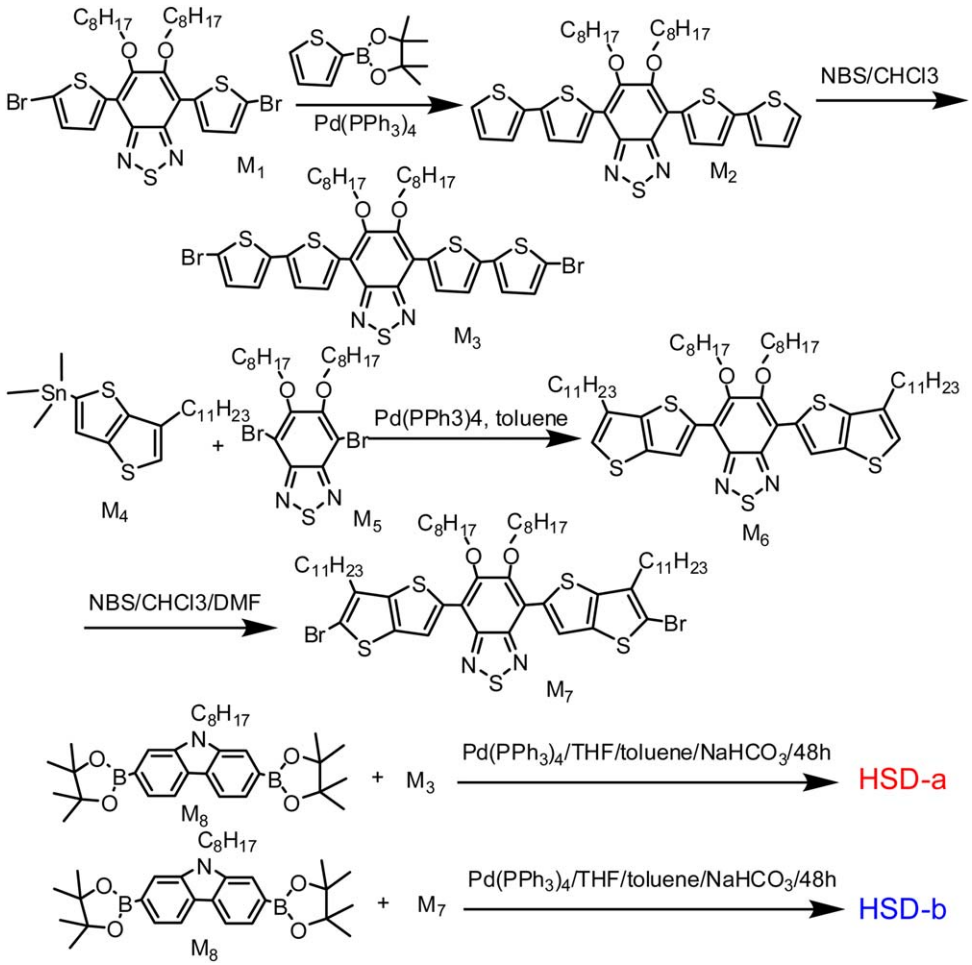

Scheme 1. Synthesis of monomers and polymers HSD-a, HSD-b. [Color figure can be viewed in the online issue, which is available at wileyonlinelibrary.com.]

in a biphasic mixture of toluene / THF and aqueous $NaHCO_3$ with freshly prepared $Pd(PPh_3)_4$ as the catalyst precursor. After polymerization for 48 h, phenylboronic acid and bromobenzene were successively added at a time interval of 12 h to cap the end of the polymers. After standard purification, polymers HSD-a and HSD-b were obtained as black solids in yields of 69% and 96%, respectively. HSD-a was almost insoluble in commonly used organic solvents such as THF, chloroform, etc. at room temperature, but it is fully soluble in 1,2-dichlorobenzene (DCB), and 1,2,4-trichlorobenzene at elevated temperature which indicates the series bithiophene π-bridge decreased solubility dramatically. The molecular weight and molecular weight distribution of HSD-a were therefore measured by gel permeation chromatography (GPC) at 150°C using 1,2,4-trichlorobenzene as an eluant calibrated with polystyrene standards and the results are summarized in Table I.

Table I. Number Average Molecular Weight (Mn), Weight Average Molecular Weight (Mw), PDI, Degradation Temperature (Td), and Glass Transition (Tg) Temperature of HSD-a, HSD-b

Polymers	Mn	Mw	PDI	Td(°C)	Tg(°C)
HSD-a	17,890	53,030	2.96	313.88	146.4
HSD-b	18,900	23,300	1.23	336.4	146.2

HSD-a possessed a Mn of 17,890 g/mol and a Mw of 53,000 g/mol with a PDI of 2.96. Compared with HSD-a, HSD-b exhibited much better solubility at room temperature and it can be dissolved in many common organic solvents. Although many fused-ring chemical compounds, such as pentacene, are generally too insoluble for device fabrication, [28,29] However, there is no the insoluble defect when planar 3-undecyl thieno[3,2-b]thiophene units was incorporated into the polymer backbone. The molecular weight and molecular weight distribution were determined by GPC using THF as the eluant and narrow distribution polystyrenes as standards at 35°C. The results showed that HSD-b possessed a Mn of 18,900 g/mol and an Mw of 23,300 g/mol with a narrow PDI of 1.23. Thermal behaviors of HSD-a and HSD-b were also investigated. As shown in Figures S1-S3 (Supporting Information), decomposition temperatures (5% weight loss) of HSD-a and HSD-b are 313 and 336°C, respectively, indicating that these two polymers are suitable for application in PSCs. An imperceptible glass transition Temperature was observed at 146.4°C for HSD-a

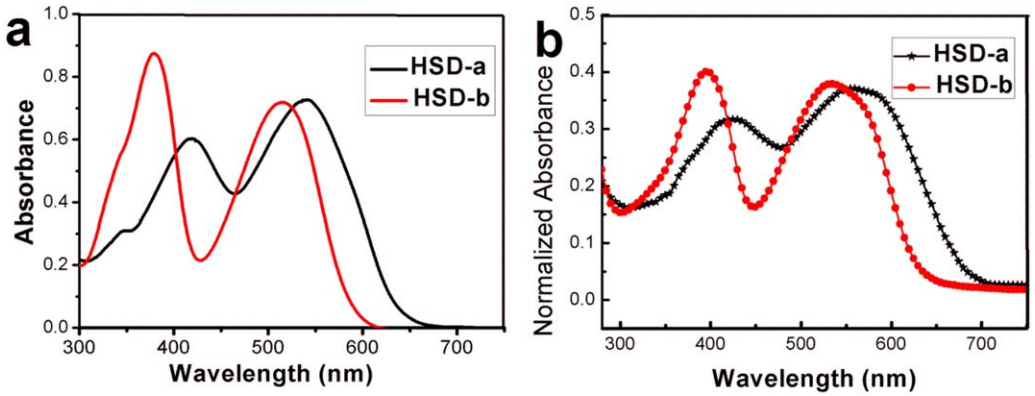

Figure 1. The absorption spectra of HSD-a, HSD-b in dilute chloroform solutions (a) and as thin film (b). [Color figure can be viewed in the online issue, which is available at wileyonlinelibrary.com.]

and 146.2°C for HSD-b in its DSC curves of the second round heating run at a rate of 10°C/min. The thermal properties of the two polymers were listed in Table I.

UV–vis absorption spectra of polymers HSD-a and HSD-b in chloroform solutions and as thin films are shown in Figure 1. In solutions, two polymers present two distinct absorption bands. The short-wavelength absorption bands located at about 420 nm for HSD-a and 367 nm for HSD-b. This peak bands originate from the π–π^* transition of the conjugated backbones, whereas the long-wavelength absorption bands peak at 542 nm for HSD-a and 515 nm for HSD-b are attributed to the internal charge transfer interaction from the donor unit to the acceptor unit. In film, the redshift compared with in the solution is attributed to the aggregation of the polymer chains in the solid state. [30,31] The two absorption bands of HSD-b became slightly broader in film, red-shifting from 367 to 396 nm and from 515 to 532 nm, respectively. Interestingly, very slight redshift of the short-wave-length peak was observed for HSD-a from 420 to 422 nm. The small redshift for the short-wavelength peak is probably due to the weak interaction of main chains in the solid state, which is probably caused by the large dihedral angle of 49.1° between the two series thiophene rings (Supporting Information Figure S12). The poor orderly π–π stacking in film for HSD-a was observed by XRD (Supporting Information Figures S6–S7). In the XRD spectra the second peak D2 clearly reveals that the distance between polymer main chains are ~0.47 nm for HSD-a and ~0.39 nm for HSD-b. The first peak d1 for HSD-a indicate ~2.3 nm distance between polymer side chains. Compared with HSD-a, a weak peak d1 of HSD-b exhibited strong disorder between polymer side chains and the distance ~0.9 nm. The long-wavelength absorption peak for HSD-a redshifts is from 542 to 570 nm. The onsets of film absorption spectra are 660 nm for HSD-a and 632 nm for HSD-b, corresponding to optical band gaps (Eg, opt) of 1.88 and 1.97 eV, respectively. Clearly, at the short-wavelength peak bands, a higher absorption ratio for HSD-b than HSD-a was found whatever in solutions or as thin films (Figure 1).

Two polymers energy levels were determined by a cyclic voltammogram (Supporting Information Figures S4 and S5). The lowest unoccupied molecular orbital (LUMO) and highest occupied molecular orbital (HOMO) were measured to be −3.56 and −5.44 eV for HSD-a; −3.66 and −5.63 eV for HSD-b. Deeper HOMO energy levels of HSD-b, can enhance the charge injection and transport properties so that it is beneficial for the high V_{oc} (0.93 V for HSD-b; 0.64 V for HSD-a). This demonstrated the principle which V_{oc} is determined by the difference between the PCBM's E_{LUMO} and the polymer's E_{HOMO} levels.[32,33]

Polymer solar cells were fabricated using HSD-a or HSD-b as electron donor and $PC_{71}BM$ as electron acceptor with a device structure of ITO/PEDOT : PSS/polymer : $PC_{71}BM$/LiF/Al. After the device optimization, solar cells fabricated with the blends of polymer and $PC_{71}BM$ in a weight ratio of 1 : 3 for HSD-a and 1 : 2 for HSD-b in ODCB solutions with the addition of 1.5% 1,8-diiodooctane (DIO) (by volume) as the additive gave the best performance. A PCE of 2.15% with a comparable V_{oc} of 0.64 V, J_{sc} of 8.75 mA/cm^2, and FF of 0.40 for HSD-a was demonstrated. A PCE of 2.59% with a high V_{oc} of 0.93 V, a J_{sc} of 7.3 mA/cm^{-2}, and a comparable fill factor (FF) of 0.38 for HSD-b under simulated solar illumination of AM 1.5 G (100 mW/cm^2). The FF values of these two polymer solar cells are relatively low. The lower FF values maybe caused by imperfect film morphology (Figure 3). Both charge generation and recombination depend strongly on the morphology of active layer.[34]

The charge-carrier mobility of these polymers was measured by using the space-charge-limited current (SCLC) method in the direction perpendicular to the electrodes. For pure HSD-a and HSD-b the SCLC mobilities were measured to be 1.95×10^{-4} and 1.49×10^{-4} cm^2/V/s, respectively. The mobility of HSD-b is slightly lower compared with that of HSD-a, However they have the same order of magnitude (Supporting Information Figures S10 and S11).

The typical current density–voltage (J–V) curves of solar cells with the blends of HSD-a:$PC_{71}BM$ (1 : 3, by weight) or HSD-b:$PC_{71}BM$ (1 : 2, by weight) as the active layer are shown in Figure 2(a). The typical feature of HSD-b-based solar cells is their high V_{oc}, indicating that the 3-undecylthieno[3,2-b]thiophene-containing polymers are promising donor materials for polymer using in tandem PSCs.

External quantum efficiency (EQE) curves of HSD-a:$PC_{71}BM$ (1 : 3, by weight) and HSD-b:$PC_{71}BM$ (1 : 2, by weight) based

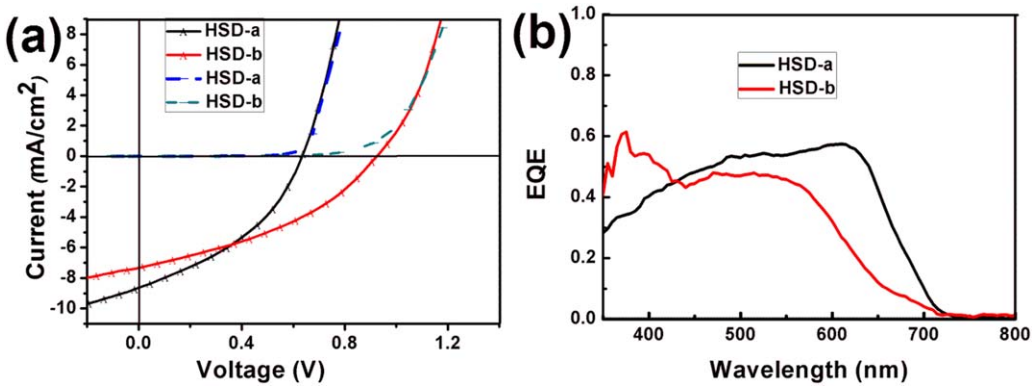

Figure 2. (a) J-V characteristics under white light illumination (solid lines) and in dark (dashed lines) of HSD-a:$PC_{71}BM$ (1 : 3, by weight) and HSD-b:PC_{71} BM (1 : 2, by weight). (b) EQE curves of the same devices. [Color figure can be viewed in the online issue, which is available at wileyonlinelibrary.com.]

PSCs are shown in Figure 2(b). Polymer HSD-a gives lower V_{oc} than that of HSD-b due to the lower oxidation potential, but their current density is consistently enhanced. Significantly, broader photocurrent responses from 320 to 720 nm than the corresponding absorption spectra (Figure 1) can be observed for HSD-a and HSD-b-based solar cells. The broad absorption of $PC_{71}BM$ can compensate the absorption valley of the polymers and the contribution from $PC_{71}BM$ to the photocurrent is very important. Significant feature for HSD-b-based solar cells is the higher EQE value between 320 nm to 450 nm and this will be great beneficial for the front cell of the tandem structure devices. The current density (J_{sc}) values calculated from the integration of EQEs (for HSD-a: 10 mA/cm^2; for HSD-b: 7.6 mA/cm^2) agree roughly with the J_{sc} values (for HSD-a: 8.8 mA/cm^2; for HSD-b: 7.3 mA/cm^2) obtained from the J-V measurements.[35] The morphology of polymer:$PC_{71}BM$ blend film, which is closely related to the device performance of BHJ PSCs, was investigated by scanning electron microscope (SEM) and atomic force microscopy (AFM) using tapping mode. For an ideal active layer structure of BHJ PSCs, an interpenetrating bicontinuous network for polymer and $PC_{71}BM$ with the domain size of 10–20 nm is desirable.[36] As shown in Figure 3, Supporting Information Figures S8 and S9, the topographies of the two polymer blends show significantly different height images. The HSD-a: $PC_{71}BM$ blend film spin-coated from ODCB solutions has much rougher surface with larger aggregations. The root-mean-square (RMS) roughness value is about 8.71 nm. This indicates compact chain packing for HSD-a so it brings about a slight enhancement of photocurrent. The HSD-b: $PC_{71}BM$ blend film spin-coated from ODCB solutions exhibited relatively smooth surface without apparent large aggregations formation and the RMS roughness value is about

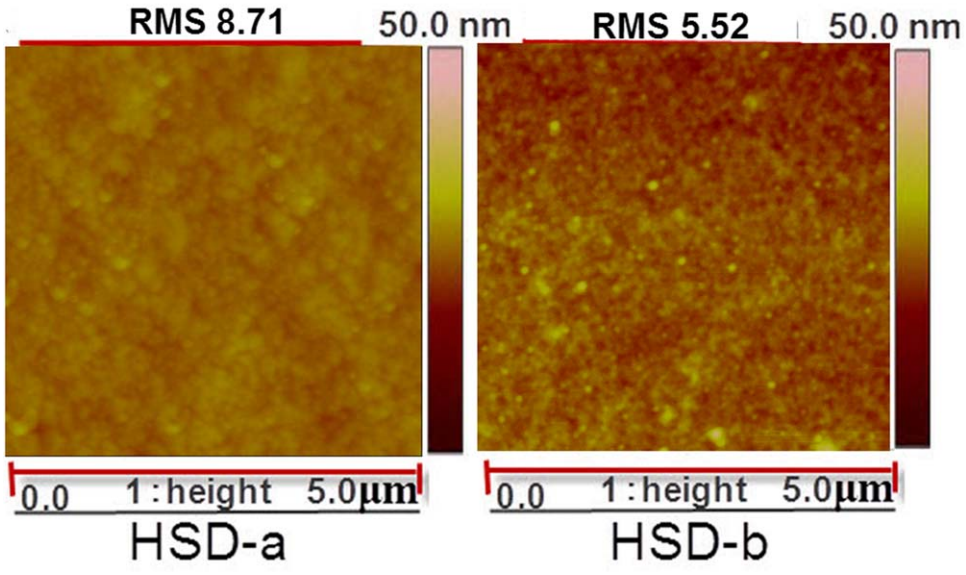

Figure 3. AFM images (5 × 5 μm^2) of the blends of polymer:$PC_{71}BM$ (1 : 3, by weight) spin-coated from ODCB solutions (containing 1.5% DIO in volume). [Color figure can be viewed in the online issue, which is available at wileyonlinelibrary.com.]

5.52 nm. The good solubility for HSD-b was believed the major reason for smaller aggregations.

CONCLUSIONS

Two D-π-A alternating conjugated polymers HSD-a and HSD-b have been designed and synthesized. Different π-bridges units crucially influence the polymer film morphology and optical, electrochemical, charge transport and photovoltaic properties. A fused-ring bithiophene π-bridge adorned with certain alkyls side chain (polymer: HSD-b) can achieve higher PCE value than a series bithiophene π-bridge without alkyls side chain (polymer: HSD-a). The polymer HSD-b has a wider band gap of about 1.97 eV. A PCE of 2.59%, with a higher V_{oc} of 0.93 V, a moderate J_{sc} of 7.3 mA/cm^2, and a comparable FF of 0.38, has been achieved in simply processed devices. HSD-b is a promising polymer for tandem PSCs as the front cell for its higher EQE value between 320 nm to 450 nm and higher V_{oc} value up to 0.93 V.

ACKNOWLEDGMENTS

This work was financially supported by the Postdoctoral Starting Foundation of Henan Normal University (01026500105); Young Scientists Foundation of Henan Normal University (01026400061); NSFC (11074066) and Henan Province basic and frontier technology research projects (1323004100247). The authors are grateful to Prof. Zhishan Bo of Beijing Normal University for useful discussions.

REFERENCES

1. Qin, R.; Li, W.; Li, C.; Du, C.; Veit, C.; Schleiermacher, H.-F.; Andersson, M.; Bo, Z.; Liu, Z.; Inganäs, O.; Wuerfel, U.; Zhang, F. *J. Am. Chem. Soc.* **2009**, *131*, 14612.
2. Coughlin, J. E.; Henson, Z. B.; Welch, G. C.; Bazan, G. C. *Acc. Chem. Res.* **2014**, *47*, 257.
3. Chen, Y.; Wan, X.; Long, G. **2013**, *46*, 2645.
4. Chen, J.; Cao, Y. *Acc. Chem. Res.* **2009**, *42*, 1709.
5. Wang, E.; Ma, Z.; Zhang, Z.; Vandewal, K.; Henriksson, P.; Inganäs, O.; Zhang, F.; Andersson, M. R. *J. Am. Chem. Soc.* **2011**, *133*, 14244.
6. Li, K.; Li, Z.; Feng, K.; Xu, X.; Wang, L.; Peng, Q. *J. Am. Chem. Soc.* **2013**, *135*, 13549.
7. Osaka, I.; Kakara, T.; Takemura, N.; Koganezawa, T.; Takimiya, K. *J. Am. Chem. Soc.* **2013**, *135*, 8834.
8. Son, H. J.; Wang, W.; Xu, T.; Liang, Y.; Wu, Y.; Li, G.; Yu, L. *J. Am. Chem. Soc.* **2011**, *133*, 1885.
9. He, Z.; Zhong, C.; Su, S.; Xu, M.; Wu, H.; Cao, Y. *Nat. Photon* **2012**, *6*, 591.
10. Li, W.; Furlan, A.; Hendriks, K. H.; Wienk, M. M.; Janssen, R. A. J. *J. Am. Chem. Soc.* **2013**, *135*, 5529.
11. You, J.; Dou, L.; Yoshimura, K.; Kato, T.; Ohya, K.; Moriarty, T.; Emery, K.; Chen, C.-C.; Gao, J.; Li, G.; Yang, Y. *Nat. Commun.* **2012**, *4*, 1446.
12. Liu, M.; Johnston, M. B.; Snaith, H. J. *Nature* **2013**, *501*, 395.
13. Chen, Q.; Zhou, H.; Hong, Z.; Luo, S.; Duan, H.-S.; Wang, H.-H.; Liu, Y.; Li, G.; Yang, Y. *J. Am. Chem. Soc.* **2014**, *136*, 622.
14. Jeon, N. J.; Lee, J.; Noh, J. H.; Nazeeruddin, M. K.; Grätzel, M.; Seok, S. I. *J. Am. Chem. Soc.* **2013**, *135*, 19087.
15. http://www.heliatek.com; Heliatek GmbH: Dresden, Germany (Last accessed on: May 5, 2013).
16. Gong, X.; Li, C.; Lu, Z.; Li, G.; Mei, Q.; Fang, T.; Bo, Z. *Macromol. Rapid Commun.* **2013**, *34*, 1163.
17. Li, G.; Zhu, R.; Yang, Y. *Nat. Photon* **2012**, *6*, 153.
18. Dennler, G.; Scharber, M. C.; Ameri, T.; Denk, P.; Forberich, K.; Waldauf, C.; Brabec, C. J. *Adv. Mater.* **2008**, *20*, 579.
19. Huang, F.; Chen, K.-S.; Yip, H.-L.; Hau, S. K.; Acton, O.; Zhang, Y.; Luo, J.; Jen, A. K. Y. *J. Am. Chem. Soc.* **2009**, *131*, 13886.
20. Blouin, N.; Leclerc, M. *Acc. Chem. Res.* **2008**, *41*, 1110.
21. Qin, R.; Bo, Z. *Macromol. Rapid Commun.* **2012**, *33*, 87.
22. Shi, S.; Jiang, P.; Chen, S.; Sun, Y.; Wang, X.; Wang, K.; Shen, S.; Li, X.; Li, Y.; Wang, H. *Macromolecules* **2012**, *45*, 7806.
23. Wang, X.; Sun, Y.; Chen, S.; Guo, X.; Zhang, M.; Li, X.; Li, Y.; Wang, H. *Macromolecules* **2012**, *45*, 1208.
24. Qin, R.; Jiang, Y.; Ma, H.; Yang, L.; Liu, H.; Chang, F. *J. Appl. Polym. Sci.* **2013**, *129*, 2671.
25. Zhang, X.; Köhler, M.; Matzger, A. J. *Macromolecules* **2004**, *37*, 6306.
26. Bouffard, J.; Swager, T. M. *Macromolecules* **2008**, *41*, 5559.
27. Tolman, C. A.; Seidel, W. C.; Gerlach, D. H. *J. Am. Chem. Soc.* **1972**, *94*, 2669.
28. Lei, T.; Wang, J.-Y.; Pei, J. *Acc. Chem. Res.* **2014**, *47*, 1117.
29. Zhang, Q.; Peng, H.; Zhang, G.; Lu, Q.; Chang, J.; Dong, Y.; Shi, X.-Y.; Wei, J.-F. *J. Am. Chem. Soc.* **2014**, *136*, 5057.
30. Qin, R. P.; Song, G. L.; Jiang, Y. R.; Bo, Z. S. *Chem. J. Chin. Univ.-Chin.* **2012**, *33*, 828.
31. Du, C.; Li, C.; Li, W.; Chen, X.; Bo, Z.; Veit, C.; Ma, Z.; Wuerfel, U.; Zhu, H.; Hu, W.; Zhang, F. *Macromolecules* **2011**, *44*, 7617.
32. Dennler, G.; Scharber, M. C.; Brabec, C. J. *Adv. Mater.* **2009**, *21*, 1323.
33. Huo, L.; Zhang, S.; Guo, X.; Xu, F.; Li, Y.; Hou, J. *Angew. Chem. Int. Ed.* **2011**, *50*, 9697.
34. Li, W.; Zhou, Y.; Viktor Andersson, B.; Mattias Andersson, L.; Thomann, Y.; Veit, C.; Tvingstedt, K.; Qin, R.; Bo, Z.; Inganäs, O.; Würfel, U.; Zhang, F. *Org. Electronics* **2011**, *12*, 1544.
35. Kumar, P.; Chand, S. *Progr. Photovoltaics Res. Appl.* **2012**, *20*, 377.
36. Blom, P. W. M.; Mihailetchi, V. D.; Koster, L. J. A.; Markov, D. E. *Adv. Mater.* **2007**, *19*, 1551.